Accurate Derivation of Chaos-Based Acquisition Performance in a Fading Channel

Ramin Vali, *Student Member, IEEE*, Stevan Berber, *Senior Member, IEEE*, and Sing Kiong Nguang, *Senior Member, IEEE*

***Abstract*—Accurate expressions for sequence acquisition in a chaos-based spread-spectrum system are derived using the statistical properties of the chaos-based spreading sequences. The expressions are validated by comparing the analytical predictions of the acquisition performance with the simulation results for three channel scenarios. Additive white Gaussian noise and Rayleigh fading channels are considered in the first two scenarios. As the third scenario a blind chip interleaving serial search algorithm is proposed and system performance is shown to improve. The simulation results show excellent agreement with the theoretical results for all three scenarios considered. This is significant as previous examinations of the same have only yielded upper-bounds.**

***Index Terms*—Synchronization, acquisition, chaotic correlation characterization, fading, chaos-based communications.**

I. Introduction

THE use of chaos-based signals in digital communications was suggested in 1992 [1], and since then many different transmission and detection techniques have been proposed [2]–[4]. Some of the earlier works have been primarily concerned with the use of the synchronization between chaotic attractors as information carriers [1], [5], [6]; however, it has been shown that these methods do not offer a level of robustness suitable for practical applications. More recent works have concentrated using chaos-based signals to transmit and detect messages [7]–[13] with encouraging results in terms of robustness.

It has been shown that chaos-based communication systems are potentially advantageous in terms of security [14], ease of wide-band signal generation [2], [14] and orthogonality [15]–[17]. These characteristics make them desirable in a wide-band digital communications context. One way of employing chaos-based signals in digital communications is to use them as spreading sequences in Direct Sequence Spread Spectrum (DS-SS) communications, which was first proposed in [18]. Chaos-based spreading sequences are wide-band, random-like, theoretically aperiodic sets of values generated using discrete representations of chaotic dynamical systems known as *chaotic maps* [17]. These sequences show high sensitivity to initial conditions, and many uncorrelated spreading sequences maybe generated using the same chaotic map [17]. Mazzini *et al.* and Rovatti *et al.* have shown that using a slice of quantized periodically repeated chaos-based spreading sequence can improve the capacity and decrease the bit-error-rate (BER) of chaos-based spread spectrum systems [15], [19].

Chaos-based digital communication techniques can be organized into two broad categories [2]. The first is the non-coherent technique, in this case the system does not rely on a replica of the transmitter spreading sequence to be available at the receiver [17]. Different single- and multi-user schemes have been suggested for the non-coherent technique, most involving the transmission of a reference alongside the transmitted signal [2], [13], [20]–[22]. The second category is the coherent technique, which relies on the exact replica of the transmitter spreading sequence being available at the receiver [5], [18], [23]–[25]. The coherent technique also requires the transmitter and receiver spreading sequences to be synchronized [26]. Synchronization for DS-SS systems is typically broken into two distinct phases known as acquisition and tracking [26]. Tracking for chaos-based DS-SS systems has been covered extensively in [8], [9] and will not be discussed here. It also has to be noted that the sequences generated by a Logistic map are real and this poses implementation problems since the sequences generated have to be quantized to be used in a hardware implementation.

The acquisition of chaos-based spreading sequences is a non-trivial problem [2], [17], [27]–[31]. Acquisition techniques for chaos-based spreading sequences presented in the literature use conventional DS-SS synchronization techniques, the most popular of which is the serial search algorithm explained in [26]. The serial search algorithm involves searching through all possible phase delays of a pilot sequence for the highest correlation value. The phase delay with the highest correlation value is assumed to be synchronized to the incoming pilot sequence [26].

In order to analyze the performance of a chaos-based serial search algorithm the cross- and auto-correlation functions of the chaotic spreading sequences have to be considered. Usually, the cross- and auto-correlation functions of the chaos-based spreading sequences are assumed to be constant, irrespective of an individual sequence's time series [7], [18], [32]–[38]. For example, [18] states that the correlation properties of chaos-based and binary spreading sequences are the same; [32] presents a system based on the same assumption, and only gives an upper-bound for acquisition performance; [33], [34], [39] assume the chaos-based correlation function remains constant, although the sequence changes, and apply the conventional synchronization derivation formulae. [7] has

Manuscript received February 17, 2011; revised July 25, 2011; accepted October 14, 2011. The associate editor coordinating the review of this letter and approving it for publication was Prof. G. Colavolpe.

The authors are with the Department of Electrical and Computer Engineering, The University of Auckland New Zealand, Private Bag 92019 Auckland Mail Centre Auckland 1142 New Zealand (e-mail: r.vali@ieee.org, {s.berber, sk.nguang}@auckland.ac.nz).

Digital Object Identifier 10.1109/TWC.2011.120511.110306

performed an analysis of acquisition in a fading channel, but only upper-bounds are given; and [35] proposes synchronization techniques for chaos-based systems but (in this case) the pilot is binary. The variable correlation function issue is partly addressed in [37], [38], where the authors examine the cross- but not the auto-correlation function. The work presented in [23] has also highlighted this issue; however, [23] only considered attractor-based basis functions, and not chaos-based spreading sequences generated from chaotic maps.

The need for an accurate theoretical model for performance evaluation of chaos-based serial search algorithm — which takes into account the statistical variability of the correlation function — has motivated the authors to offer this contribution. Since synchronization analysis is fundamentally a statistical problem [40], a statistical approach for modeling the chaos-based cross- and auto-correlation functions has been chosen. The resulting model is then used to evaluate the serial search acquisition performance of a chaos-based DS-SS system, without the need for approximations or upper-bounds, and this is the primary contribution of this paper. In order to establish the validity of the approach, three separate scenarios involving noise, fading, and blind chip inter-leaving are considered. As a secondary contribution, we present the use of the blind chip inter-leavers which, to the authors' knowledge, have not been considered for the serial search algorithm. The theoretical analysis is supported by numerical results.

The reminder of this paper is organized as follows. Section II presents the statistical framework used to examine the correlation functions of chaos-based spreading sequences. Section III gives an overview of the acquisition technique examined. Section IV addresses the three scenarios used to validate the statistical framework, and presents intermediate statistical results. Section V presents the final theoretical and simulation results in terms of the acquisition phase performance and discusses these results. Section VI concludes the paper.

II. Statistical Characterization of Chaos-based Correlation Function

The chaotic pilot sequence used in this paper is generated using the Logistic map, which is an example of iterative form for generating discrete chaotic sequences. The Logistic map has been used in other investigations before, and it is shown in [7] that the sequences generated from this map are orthogonal. The iterative function is $x_{n+1} = 2x_n^2 - 1$ [41], and is bounded between $(-1, 1)$. The initial conditions for this map can be any value within $(-1, 1)$ except $\frac{-1}{2}$, $\frac{1}{2}$ and 0. Considering the probability density function (PDF) of the Logistic map given by [41],

$$P_x(x) = \frac{1}{\pi\left(\sqrt{1-x^2}\right)}, \quad (-1 < x < 1), \tag{1}$$

the values for the mean and variance of the Logistic map can be calculated as 0 and $\frac{1}{2}$ respectively.

The correlation function of the chaotic pilot sequence is given by,

$$z[j] = \sum_{i=1}^{L} \left(x_{i-\tau} x_{i-j}\right), \tag{2}$$

where z is the discrete correlation result, j is the time index of the correlation i.e. the phase delay corresponding to the locally generated chaotic pilot sequence, τ is the time lag between the two sequences due to propagation, and L is the number of chips in the correlation. Over a large set generated using different initial conditions, it can be assumed each $x_{i-\tau}$ and x_{i-j}, are random variables with PDFs given by (1). As a result, the correlation output can be considered a random variable consisting of the summation of the product of the two chaotic sequences over L chips. If L is a small value, the correlation function will not follow a Gaussian distribution [42]. However, given L is usually more than 50 chips for typical schemes [7], it can be assumed the correlation function is the sum of a large number of independent, identically distributed random variables, and therefore can be accurately modeled by a Gaussian distribution. Two possibilities arise ; first, $j \neq \tau$ which corresponds to the two chip sequences being out of synchrony. Since chaotic sequences are orthogonal, this corresponds to the cross-correlation of the two sequences. Therefore, for h trials, the correlation result for non-aligned sequences is a Gaussian random variable Z_{h_0}, where $\mathrm{Z}_{h_0} \sim \mathrm{G}\left(0, \frac{L}{4}\right)$. The second possibility is $j = \tau$, which corresponds to the auto-correlation peak of the two sequences. For h trials, the correlation result for aligned sequences can be assumed to be a Gaussian random variable corresponding to the variation of the auto-correlation peak, given by $\mathrm{Z}_{h_1} \sim \mathrm{G}\left(\frac{L}{2}, \frac{L}{8}\right)$. The subscripts h_o and h_1 refer to the non-synchronized and synchronized hypotheses respectively. Fig. 1 shows a comparison between the statistical models proposed and the computed distributions of Z_{h_0} and Z_{h_1}. The average error between the distributions and the statistical models is also shown verifying the statistical characterization presented.

The Logistic map is from the family of Chebychev maps all of which have the same PDF given by (1) [41]. So if any of the maps from the Chebychev family are used, the analysis presented in this paper can be readily applied. If other chaotic maps with different statistical properties are used, the general approach used in this paper can still be applied to them if a large correlation length ($L > 20$) is used, the mean and variances of the Gaussian distributions have to be recalculated however.

Our investigation indicates that, with a sufficiently large correlation length, the cross- and auto-correlation peaks are not constant, but follow Gaussian distributions. This way of examining chaos-based correlation functions has not been applied before, to the authors' knowledge, and will have implications on all subsequent investigations involving chaos correlation functions.

III. System Description

The acquisition block diagram is shown in Fig. 2. The transmitter sends a periodic chaotic chip sequence as the pilot signal, which is time delayed by a random propagation delay τ, and corrupted in the wireless channel. This pilot is modulated by a continuous set of +1 bits. Normally, the time delay between the transmitter and receiver is not an exact multiple of the chip duration. However, the role of the acquisition is to find the time delay to the nearest chip [43]. The rest of the operation will be handled by the tracking

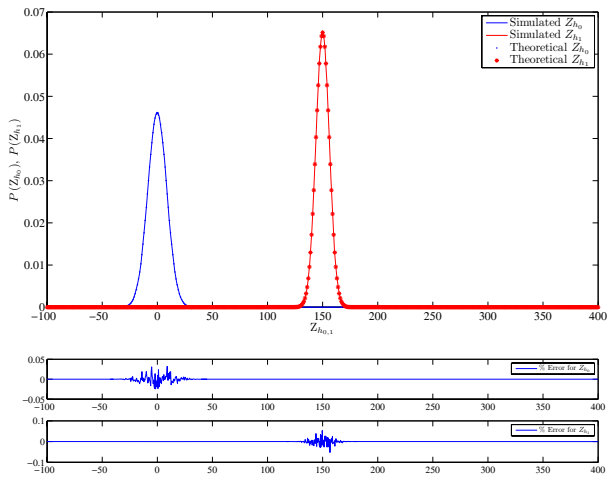

Fig. 1. Comparison between the statistical models and simulated distributions of Z_{h_0} and Z_{h_1}.

phase described in [8], [43]. Therefore τ is assumed to be a multiple of the chip duration for acquisition for the purposes of this paper. The receiver has an exact replica of the transmitted pilot; however, due to the propagation delay, the two sequences are not aligned in time (synchronized). A sliding correlator, a square law device and a thresholder in a loop formation are used to perform the signal acquisition. The sliding correlator can perform correlation on all, or a fraction, of the pilot sequence. Once the output of the square law device exceeds the threshold Z_{Th}, synchronization is declared and the system will enter the tracking mode. If the synchronization is lost whilst the system is in the tracking mode, i.e. when information is being transmitted, the system reverts back to acquisition and the synchronization process will restart.

A representation of the output of the square-law device is shown in Fig. 3. Given synchronization is an inherently statistical process, a probability can be assigned to the squared correlation peak being placed at the correct time delay index $j = \tau$ (Fig. 3). This is the *probability of detection,* $P_{_D}$. On the other hand, it can be seen that there are two other peaks at incorrect time delay indices with values over Z_{Th}. The probability assigned to such an event which is known as the *probability of false alarm* or $P_{_F}$. The performance measures used for this investigation are $P_{_D}$ and $P_{_F}$ which will be accurately derived as the primary contribution of this paper.

It is assumed the wireless channel is corrupted by noise taken from a zero mean, additive white Gaussian noise (AWGN) process, with power $\sigma_n^2 = \frac{N_o}{2}$, where N_o is the noise power spectral density. In this paper, the noise term is defined by n, where $n \sim G\left(0, \sigma_n^2\right)$. The fading coefficients given by a, and are assumed to follow a Rayleigh distribution, $f_A\left(a\right) = \frac{a}{b^2} \exp\left(-\frac{a^2}{2b^2}\right)$, where b is the mode of the Rayleigh distribution chosen in such a way to make $\mathrm{E}\left[a^2\right] = 1$ [44]. The duration of the fading coefficients are generally larger than a chip period and normally are as long as a bit interval [44]. As a result, it is assumed the fading coefficients change every bit period [44], this assumption allows for a mathematically tractable analysis.

The investigation presented in this paper is performed in base-band; however, the extension to pass-band would be relatively simple as the effect of the square law device on the correlation function is already considered. If the square law devise is not taken into account the derivation of $P_{_D}$ and $P_{_F}$ will become simpler; however, the results obtained cannot be extended to a pass-band case. As a result, the approach in this paper is to take into account the square law device which will be used in a pass-band system to eliminate the phase difference between the incoming and locally generated carriers. Also, it is assumed that other users are not transmitting at the time of acquisition. Therefore inter-user interference (IUI) is not considered in this paper; however, once the proposed acquisition model is in place, the IUI can be considered as additive noise [7].

IV. Derivation of $P_{_D}$ and $P_{_F}$

This section presents three scenarios in which the chaos-based acquisition has to estimate the time delay between the transmitted and received pilots. The performance measures in the form of $P_{_D}$ and $P_{_F}$, are then derived and compared for each scenario. The three scenarios are: acquisition in presence of noise, acquisition in presence of noise and Rayleigh multi-path fading, and acquisition in presence of noise and Rayleigh multi-path fading using interleavers.

A. Acquisition in Presence of Noise

The block diagram for this scenario can be visualized by omitting the fading coefficients and interleaver/de-interleaver pair from the acquisition block diagram shown in Fig. 2. Given the system is only corrupted by noise, the received signal can be written as $r_i = x_{i-\tau} + n_i$, which after correlation with the local replica can be written as,

$$z\left[j\right] = \sum_{i=1}^{L} \left(x_{i-\tau} x_{i-j}\right) + \sum_{i=1}^{L} \left(n_i x_{i-j}\right), \tag{3}$$

which is one realization of random variable Z_h.

For the non-synchronized case

$$\mathrm{Z}_{h_0} \sim G\left(0, \frac{L}{4} + \frac{L\sigma_n^2}{2}\right), \tag{4}$$

and for the synchronized case

$$\mathrm{Z}_{h_1} \sim G\left(\frac{L}{2}, \frac{L}{8} + \frac{L\sigma_n^2}{2}\right). \tag{5}$$

where $\frac{L\sigma_n^2}{2}$ is the contribution of the noise term to the variance of the total signal as shown in Appendix A.

The effect of the square law device on the correlation output can be considered by squaring the variables given in (4) and (5), and normalizing against the variance of Z_{h_0} and Z_{h_1} respectively. Therefore,

$$p\left(\mathrm{Z}'_{h_0}, 1\right) = \frac{1}{\sqrt{2\pi \mathrm{Z}'_{h_0}}} \exp\left(\frac{-\mathrm{Z}'_{h_0}}{2}\right), \tag{6}$$

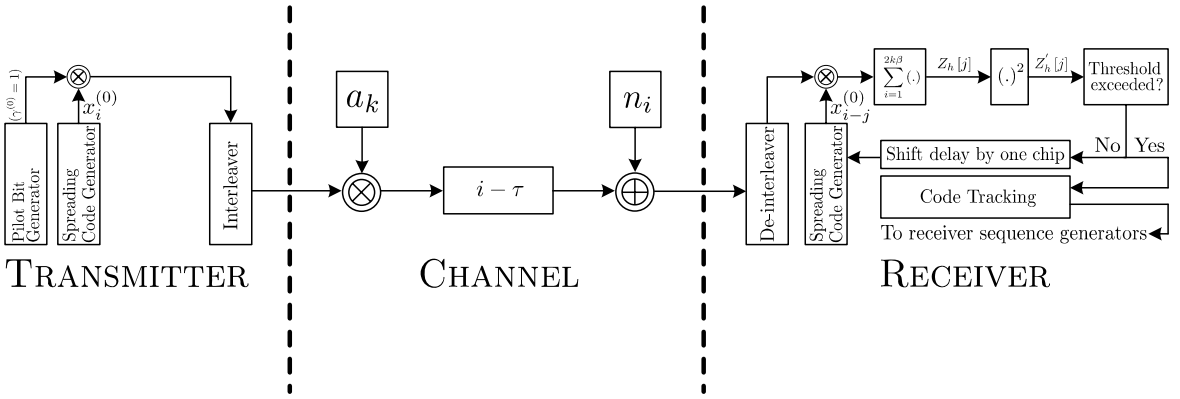

Fig. 2. Simplified base-band equivalent of a DS-SS acquisition phase with noise and multi-path fading

where $\mathrm{Z}'_{h_0} = \frac{\mathrm{Z}^2_{h_0}}{\sigma^2_{\mathrm{Z}_{h_0}}}$ is the squared and normalized random variable, and follows a chi-square distribution.

Similarly,

$$p\left(\mathrm{Z}'_{h_1}, 1, \lambda\right) = \frac{1}{2}\exp\left(\frac{-\left(\mathrm{Z}'_{h_1}+\lambda\right)}{2}\right)\left(\frac{\mathrm{Z}'_{h_1}}{\lambda}\right)^{-\frac{1}{4}} \times \mathrm{I}_{-\frac{1}{2}}\left(\sqrt{\mathrm{Z}'_{\mathrm{h}_1}\lambda}\right) \quad (7)$$

which follows a non-central chi-square distribution with the non-centrality parameter λ, $\mathrm{Z}'_{h_1} = \frac{\mathrm{Z}^2_{h_1}}{\sigma^2_{\mathrm{Z}_{h_1}}}$, and $\mathrm{I}(.)$ is a modified Bessel function of the first kind. The non-centrality parameter can be expressed as

$$\lambda_{\mathrm{Noise}} = \frac{2L}{1+4\sigma_n^2}, \quad (8)$$

which is derived in Appendix A.

Fig. 4 presents a comparison between the statistical model given by (6) and (7) with the computed distributions of $Z'_{h_{0,1}}$ and error bars for both cases. The results show close agreement, verifying this particular approach.

Fig. 5 gives a visual representation of the method used to determine $P_{_D}$ and $P_{_F}$ from (6) and (7).

As shown in Fig. 5, $P_{_F}$ is the area under $p\left(\mathrm{Z}'_{h_0}, 1\right)$ from the preset threshold Z_{Th} up to infinity. Similarly $P_{_D}$ is the area under $P\left(\mathrm{Z}'_{h_1}, 1, \lambda\right)$ from Z_{Th} to infinity. As a result, $P_{_F}$ and $P_{_D}$ can be expressed as

$$P_{_F} = \int_{Z_{Th}}^{\infty} p\left(\mathrm{Z}'_{h_0}, 1\right) d\mathrm{Z}'_{h_0} = 1 - \mathrm{erf}\left(\frac{\sqrt{Z_{Th}}}{\sqrt{2}}\right), \quad (9)$$

$$P_{_D} = \int_{Z_{Th}}^{\infty} p\left(\mathrm{Z}'_{h_1}, 1, \lambda\right) d\mathrm{Z}'_{h_1} = 1 - \frac{\mathrm{erf}\left(\sqrt{\frac{Z_{Th}}{2}} - \sqrt{\frac{\lambda}{2}}\right)+}{2} \frac{\mathrm{erf}\left(\sqrt{\frac{Z_{Th}}{2}} + \sqrt{\frac{\lambda}{2}}\right)}{2}, \quad (10)$$

which are derived in Appendix B.

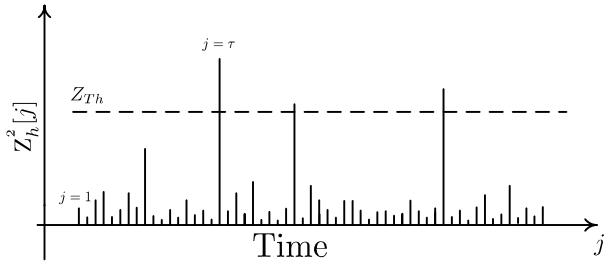

Fig. 3. Output of the square-law device and thersholding.

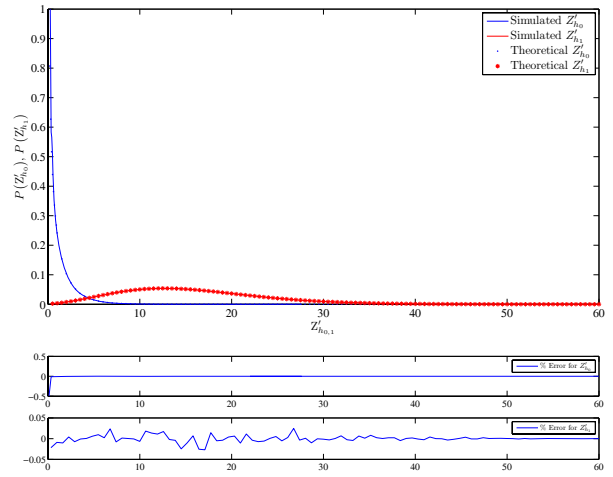

Fig. 4. Comparison between the statistical models and simulated distributions of Z'_{h_0} and Z'_{h_1}.

B. Acquisition in Presence of Noise and Rayleigh Multi-path Fading

In this scenario, it is assumed the transmitter pilot is affected by slow Rayleigh fading. The block diagram can be visualized by omitting the interleaver/de-interleaver pair from Fig. 2. The number of chips (L) in the pilot is typically a multiple of the spreading factor (2β). Since the fading coefficients change

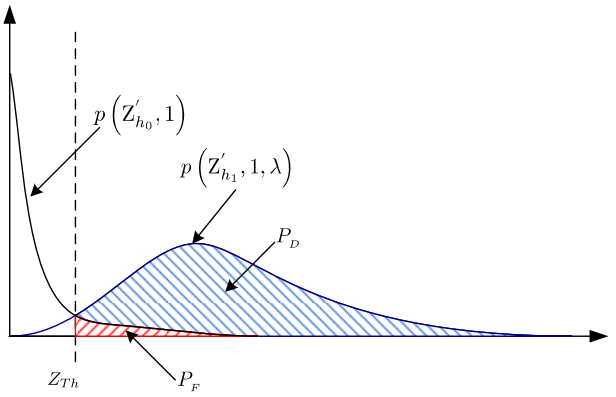

Fig. 5. Visual representation of P_D and P_F based on $P\left(\mathrm{Z}'_{h_0},1\right)$ and $P\left(\mathrm{Z}'_{h_1},1,\lambda\right)$.

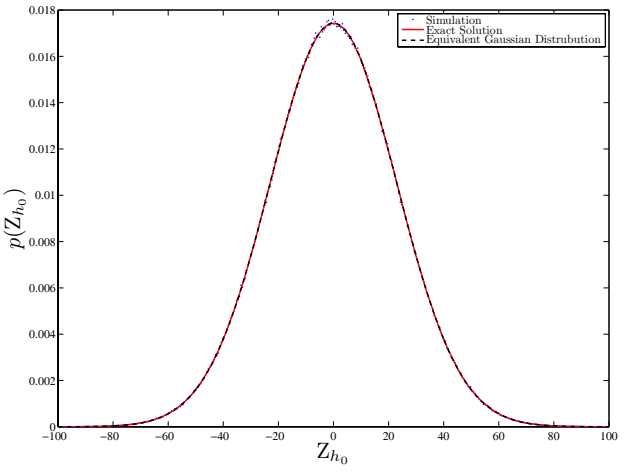

Fig. 6. Comparison between the exact distribution of Z given in (12), Gaussian approximation and simulation.

every bit, the correlator output is

$$z\left[j\right] = \underbrace{a_1 \sum_{i=1}^{L}\left(x_{i-\tau}x_{i-j}\right)+\sum_{i=1}^{L}\left(n_i x_{i-j}\right)+}_{\text{Bit 1}}$$

$$\underbrace{a_2 \sum_{i=2\beta+1}^{2L}\left(x_{i-\tau}x_{i-j}\right)+\sum_{i=2\beta+1}^{2L}\left(n_i x_{i-j}\right)+\ldots}_{\text{Bit 2}}$$

$$\underbrace{+\,a_k \sum_{i=2\beta(k-1)+1}^{Lk}\left(x_{i-\tau}x_{i-j}\right)+\sum_{i=2\beta(k-1)+1}^{Lk}\left(n_i x_{i-j}\right).}_{\text{Bit } k} \tag{11}$$

Initially assuming that the pilot is one bit long, i.e. $k=1$, and if the correlation is evaluated many times using different chaotic sequences and fading coefficients, it can be written as

$$\mathrm{Z} = \mathrm{AX}+\mathrm{N}, \tag{12}$$

where Z, A, X and N are random variables representing the faded correlation function, Rayleigh fading envelope, the $\sum_{i=1}^{L}\left(x_{i-\tau}x_{i-j}\right)$ and $\sum_{i=1}^{L}\left(n_i x_{i-j}\right)$ terms respectively.

For the non-synchronized case, it has been shown in Section II that X and N have zero mean Gaussian distributions. The exact distribution of Z is given in [45]. Fig. 6 gives a comparison between the exact solution provided in [45], and a Gaussian approximation

$$\mathrm{Z}_{h_0} \sim \mathrm{G}\left(0, \frac{L}{2}\left(b^2+2\sigma_n^2\right)\right). \tag{13}$$

For $k>1$ the normalization factor changes to $\frac{kL}{2}\left(b^2+2\sigma_n^2\right)$.

The synchronized case is more involved as there are no closed form expressions for (12) when X is a non-zero mean Gaussian distribution. As a result, two different approaches are employed. The first is to hypothesize that Z_{h_1} is a Gaussian distribution. the mean and variance of this Gaussian distribution are used to find $\lambda_{\mathrm{Fading}}$ for Z'_{h_1}. The second approach is to use non-linear regression analysis to fit a distribution to Z'_{h_1}.

For the first approach, we hypothesize that for one bit

$$\mathrm{Z}_{h_1} \sim \mathrm{G}\left(\frac{Lb}{2}\sqrt{\frac{\pi}{2}}, \frac{L^2b^2}{8}\left(4-\pi\right)+\frac{L}{2}\sigma_n^2\right), \tag{14}$$

where the mean and variance have been derived in appendix C using the approach suggested in [46]. Since (14) is a non-zero mean Gaussian, the random variable Z'_{h_1} follows the same distribution given in (7). Furthermore, as the statistical properties of different pilot bits remain the same, the overall squared correlation function will be the sum of individual one bit correlation functions all squared. As a result the non-centrality parameter can be found and adjusted with a k parameter

$$\lambda_{\mathrm{Fading}} = \frac{k\pi}{\left(4-\pi\right)+\frac{2}{L}+\frac{4\sigma_n^2}{Lb^2}}. \tag{15}$$

The second approach involves using a non-linear regression method to find the best possible fit to the computation results. Using this approach, a vector for $\lambda_{\mathrm{Fading}}$ is calculated and used to predict $p\left(\mathrm{Z}'_{h_1},1,\lambda\right)$.

In order to verify the two approaches outlined, a comparison between simulations and the hypothesized and regression approaches presented in Fig. 7. It is observed that, the PDF of $p\left(\mathrm{Z}'_{h_1},1,\lambda\right)$ can be accurately predicted in the presence of noise and fading by calculating $\lambda_{\mathrm{Fading}}$ for different number of pilot bits. The average error between the simulation and the results of the statistical approach is 2.3%.

C. Acquisition in Presence of Noise and Rayleigh Multi-path Fading Using Interleavers

In this scenario the system uses a block chip interleaver de-interleaver pair to combat the effect of multi-path fading. Interleaving smears the fade power across the whole pilot sequence. The interleaver chosen in this paper is a block chip interleaver. The interleaving depth is assumed to be higher than the coherence time of the channel in such a way that

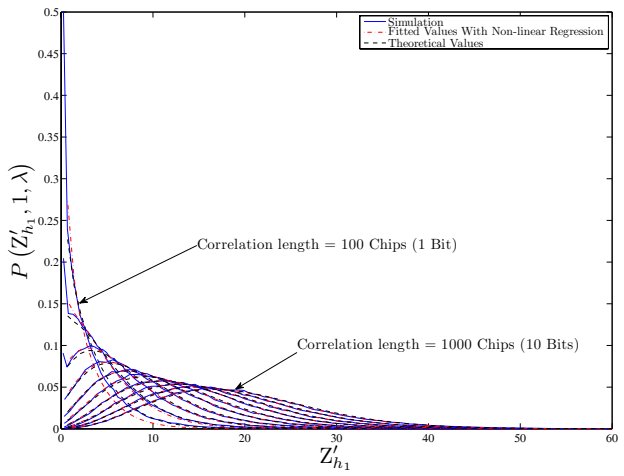

Fig. 7. Comparison between the hypothesized, non-linear regression and simulation for predicting $P\left(Z'_{h_1}, 1, \lambda\right)$.

after interleaving, the adjacent chips have different fading coefficients. This is especially effective when the pilot length is small and a good quality of synchronization is desired. At the front end of the receiver, the acquisition phase blindly de-interleaves the transmitted signal having knowledge of the bit and chip durations. It is assumed pass-band carrier synchronization has already been achieved. Initially there is no chip synchronization, so the de-interleaver will not work correctly because it performs based on faulty assumptions regarding the chip that starts a new block. The de-interleaved chip sequence is correlated with the locally generated sequence the same way as the previous two scenarios. The de-interleaving, correlation and time shifting will continue serially until the correct time shift has been reached indicating the synchronization has been achieved. In that instance, the blind de-interleaver will re-arrange the chips for every pilot bit correctly. The correlation result will then be higher than the threshold, and successful acquisition will be declared. Our aim now is to derive the performance benchmarks of $P_{_F}$ and $P_{_D}$ for this scenario and compare them to the previous two scenarios.

Given the description above, the correlator output can be expressed as

$$z[j] = \sum_{i=1}^{L} \left(a_i x_{i-\tau} x_{i-j}\right) + \sum_{i=1}^{L} \left(n_i x_{i-j}\right) \tag{16}$$

It can be shown for the non-synchronized case, as presented in appendix C, that

$$Z_{h_0} \sim G\left(0, \frac{L}{2}\left(b^2 + \sigma_n^2\right)\right). \tag{17}$$

As Z_{h_0} is a Gaussian distribution, Z'_{h_0} follows the same distribution given in (6). The only difference between the two scenarios is the variance of Z_{h_0}, which is normalized in any case.

For the synchronized case , as described in appendix D,

$$Z_{h_1} \sim G\left(\frac{Lb}{2}\sqrt{\frac{\pi}{2}}, L\left\{\frac{b^2\left(6-\pi\right) + 4\sigma_n^2}{8}\right\}\right), \tag{18}$$

which, after squaring will follow the distribution given in (7), with a non-centrality parameter of

$$\lambda_{\text{Interleaving}} = \frac{L\pi}{\left(6-\pi\right) + \frac{4\sigma_n^2}{b^2}}. \tag{19}$$

V. Results and Discussion

In the previous section, the output of the square law device was statistically modeled for different scenarios. The difference in performance between each scenario can now be predicted analytically using only the non-centrality parameter. As a result, the performance benchmarks ($P_{_F}$ and $P_{_D}$) can be calculated using the exact expressions given in (6) and (7). This section presents a comparison between the simulation results and the analytical expressions and discusses the findings.

Modeling the acquisition phase is fundamentally a statistical problem, therefore, the system was simulated using the Monte Carlo method. The square of the correlation function was computed for each trial with different spreading sequences as well as fading coefficients and noise samples. For each realization of the correlation function, a thersholding and counting operation was performed. Initially, a threshold value of zero was used and the number of false alarms $\left(Z'_{h_0} > Z_{Th}\right)$ and detections $\left(Z'_{h_1} > Z_{Th}\right)$ were recorded. The threshold was then increased by a step-size of 10, and the process was repeated. Finally the values of detections and false alarms were normalized, giving $P_{_D}$ and $P_{_F}$ respectively. The correlation length of the pilot has also been altered to observe its effects on acquisition performance. For the signal-to-noise ratio (SNR) of interest, the noise variance is adjusted by the value of the energy per bit E_b and the number of bits used in the correlator of the acquisition phase. The value of the fading mode is fixed to $b = \sqrt{\frac{1}{2}}$, causing the average power of the fading coefficients to be unity [44], [47]. It should be noted that the theoretical expressions derived in this contribution give accurate results for all values of b.

The performance of acquisition techniques are typically compared using ROC curves [7]. The simulated ROC plots are compared against the analytical results obtained by substituting the appropriate value of λ, into (10) and plotting it against $P_{_F}$ calculated from (9). Ideally, $P_{_F}$ is 0; however, a residual $P_{_F}$ exists due to noise, fading and the self-interference of chaotic sequences, the effects are particularly strong for lower values of $P_{_D}$. As a result an acceptable region of operation for acquisition is usually defined. In this paper this region of operation is $P_{_F} \in [0, 0.1]$; that is, a probability of false alarm between 0 and 10%.

The simulations are designed to verify two issues; first, that for all three scenarios considered, the analytical and approximate results agree with the simulation results; and second, to quantify the improvement gained by the chip-interleaving technique, for small correlation lengths.

Fig. 8 presents the ROC results for an SNR of 2dB and a correlation length of 100 chips. It is observed that in the region of low $P_{_F}$, ($P_{_F} \in [0, 0.1]$) the probability of detection is also low. Furthermore, as the fading coefficients reduce the correlation peak, they increase the probability of failure pulling the curves down. The interleaved result presented

show that by using chip interleaving, the performance can be improved by approximately 12% at P_F = 0.1. The maximum error between the statistical approach and simulation is 2.0%. The error is attributed to the number of trials and is expected the decrease with larger trial sets.

Fig 9 presents the ROC results for an SNR of 8dB and a correlation length of 100 chips (k= 1). The noise only result shows a significant improvement over the 2 dB result (shown in Fig. 8), as expected. However, it should be noted that the fading result has not improved significantly due to the multiplicative way fading coefficients affect correlation results. However, the improvement introduced by interleaving is significant. It is observed that the performance is improved by approximately 27%, which is significant given that the correlator has only 1 bit (100 chips) to work with. The maximum error between the statistical approach and simulation is 1.2%.

Fig 10 presents the ROC results for an SNR of 8dB and a correlation length of 300 chips (k= 3). In this case each correlation period has more than one fading coefficient. The first observation is that the performance for the fading scenario without interleaving has improved compared to Fig. 9. This is attributed to the changing of Rayleigh fading coefficients within the correlation length which reduces the adverse effects of fading on the correlation of chaotic sequence. The noise only and interleaved scenario performances have improved as expected, since there is more information available to the correlator. The maximum error between the statistical approach and simulation for this ROC result is 1.1%.

The results shown in Figs. 8, 9 and 10 are directly comparable to those presented in [7], [32], [39]. In these references, only the upper-bound results were presented.

Fig. 11 presents a 3D rendition of the percentage improvement in P_D attained by applying the interleaver for various values of k. The improvement window is widest for $P_F \in [0, 0.1]$ which is highly desirable. Also, as the value of k increases, the region of improvement decreases. However, this is of no concern as with the increase in correlation length, the performance improves. The 20-30% improvement gained for $P_F \in [0, 0.1]$ with $k < 3$ is very useful when fast synchronization is desired in a fading channel.

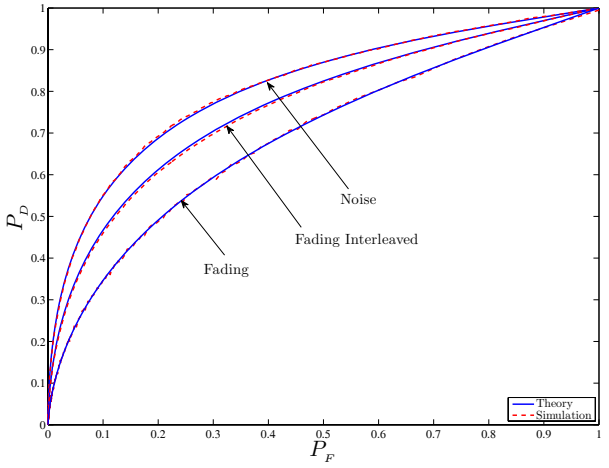

Fig. 8. ROC plot with three scenarios, for SNR = 2 dB and correlation length = 100 chips.

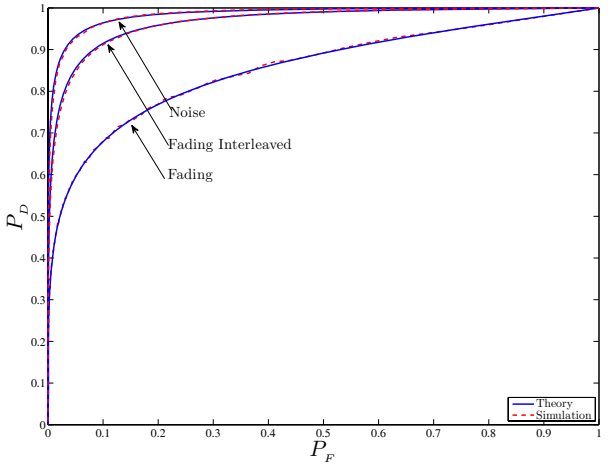

Fig. 9. ROC plot with three scenarios, for SNR = 8 dB and correlation length = 100 chips.

VI. Conclusions

In this paper, accurate expressions for the P_D and P_F for a chaos-based spread spectrum acquisition were derived using a statistical approach to the stochastic properties of the chaos-based spreading sequences. To prove the approach is valid, three different channel scenarios were considered. The analytical results show close agreement with the simulation results across all three scenarios. Also, the use of blind chip interleaving was proposed in the acquisition serial search algorithm. Analysis was performed to show a significant improvement in P_D for small correlation lengths. Overall, the statistical approach was found to be accurate and useful in other applications.

Appendix

A. Derivation of the mean and variance of Z_{h_0} and Z_{h_1} for scenario A.

$$\mathrm{E}\left[\mathrm{Z}_{h_0}\right] = \mathrm{E}\left[\sum_{i=1}^{L}\left(x_{i-\tau}x_{i-j}\right)\right] + \mathrm{E}\left[\sum_{i=1}^{L}\left(n_i x_{i-j}\right)\right] = 0.$$

$$\begin{aligned}\mathrm{Var}\left[\mathrm{Z}_{h_0}\right] &= \mathrm{Var}\left[\sum_{i=1}^{L}\left(x_{i-\tau}x_{i-j}\right)\right] + \mathrm{Var}\left[\sum_{i=1}^{L}\left(n_i x_{i-j}\right)\right] \\ &= \sum_{i=1}^{L} E\left[x_{i-\tau}^2\right] E\left[x_{i-j}^2\right] - 0 + \\ &\quad \sum_{i=1}^{L} E\left[n_i^2\right] E\left[x_{i-j}^2\right] - 0 = \frac{L}{4} + \frac{L\sigma_n^2}{2}\end{aligned}$$

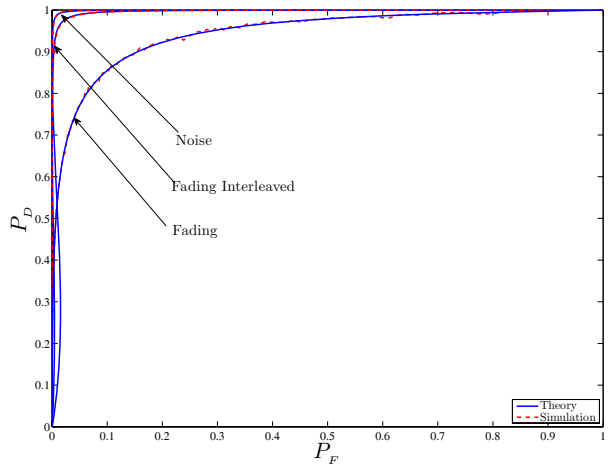

Fig. 10. ROC plot with three scenarios, for SNR = 8 dB and correlation length = 300 chips.

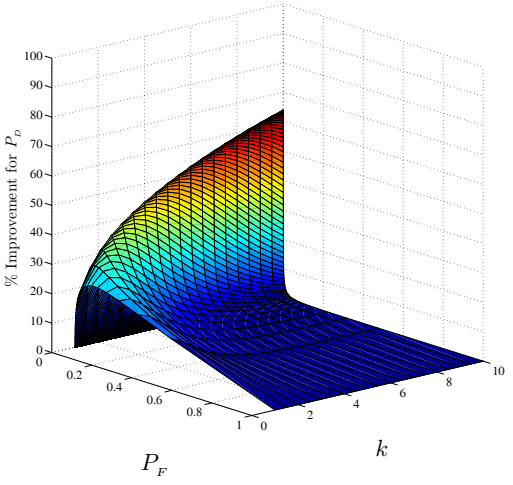

Fig. 11. Percentage improvement for P_D as a result of using the interleaver/de-interleaver pair. The improvement is measured based on the noise only performance. The SNR in this case 4 dB.

$$\begin{aligned}\mathrm{E}\left[\mathrm{Z}_{h_1}\right] &= \mathrm{E}\left[\sum_{i=1}^{L}\left(x_{i-j}x_{i-j}\right)\right]+\mathrm{E}\left[\sum_{i=1}^{L}\left(n_i x_{i-j}\right)\right]\\ &= \frac{L}{2}+0.\end{aligned}$$

$$\begin{aligned}\mathrm{Var}\left[\mathrm{Z}_{h_1}\right] &= \mathrm{Var}\left[\sum_{i=1}^{L}\left(x_{i-j}x_{i-j}\right)\right]+\mathrm{Var}\left[\sum_{i=1}^{L}\left(n_i x_{i-j}\right)\right]\\ &= \mathrm{E}\left[\sum_{i=1}^{L}\left(x_{i-\tau}^2\right)^2\right]-\mathrm{E}^2\left[\sum_{i=1}^{L}\left(x_{i-\tau}^2\right)\right]+\\ &\quad \sum_{i=1}^{L}\mathrm{E}\left[n_i^2\right]E\left[x_{i-j}^2\right]-0=\frac{L}{8}+\frac{L\sigma_n^2}{2},\end{aligned}$$

where

$$\mathrm{E}\left[\left(x_{i-\tau}\right)^4\right] = \int_{-1}^{1}x^4\frac{1}{\pi\left(\sqrt{1-x^2}\right)}dx=\frac{3}{8}$$

Derivation of λ_{Noise}

$$\lambda_{\mathrm{Noise}}=\frac{\mathrm{E}^2\left[\mathrm{Z}_{h_1}\right]}{\mathrm{Var}\left[Z_{h_1}\right]}=\frac{2L}{1+4\sigma_n^2}.$$

B. Derivation of P_D and P_F.

Derivation of P_F

$$\begin{aligned}P_F &= \int_{Z_{Th}}^{\infty}p\left(\mathrm{Z}_{h_0}^{'},1\right)d\mathrm{Z}_{h_0}^{'}\\ &= \int_{Z_{Th}}^{\infty}\frac{1}{\sqrt{2\pi\mathrm{Z}_{h_0}^{'}}}\exp\left(\frac{-\mathrm{Z}_{h_0}^{'}}{2}\right)d\mathrm{Z}_{h_0}^{'}.\end{aligned}$$

Let $\sqrt{\mathrm{Z}_{h_0}^{'}}=x\Rightarrow\frac{1}{2\sqrt{\mathrm{Z}^{'}{}_{h_0}}}d\mathrm{Z}_{h_0}^{'}=dx$ then $\frac{1}{2x}d\mathrm{Z}_{h_0}^{'}=dx\Rightarrow d\mathrm{Z}_{h_0}^{'}=2xdx$. Rewriting the integrand

$$P_F = \frac{2}{\sqrt{2\pi}}\int_{Z_{Th}}^{\infty}e^{-\frac{x^2}{2}}dx=\frac{2}{\sqrt{2\pi}}\sqrt{\frac{\pi}{2}}\mathrm{erf}\left(\frac{x}{\sqrt{2}}\right)$$

results in

$$P_F = \mathrm{erf}\left(\frac{\sqrt{\mathrm{Z}_{h_0}^{'}}}{\sqrt{2}}\right)\Bigg|_{\mathrm{Z}_{Th}}^{\infty}=1-\mathrm{erf}\left(\frac{\sqrt{\mathrm{Z}_{Th}}}{\sqrt{2}}\right).$$

Derivation of P_D

$$\begin{aligned}P_D &= \int_{Z_{Th}}^{\infty}p\left(\mathrm{Z}_{h_1}^{'},1,\lambda\right)d\mathrm{Z}_{h_1}^{'}\\ &= \int_{Z_{Th}}^{\infty}\frac{1}{2}\exp\left(\frac{-\left(\mathrm{Z}_{h_1}^{'}+\lambda\right)}{2}\right)\left(\frac{\mathrm{Z}_{h_1}^{'}}{\lambda}\right)^{-\frac{1}{4}}\times\\ &\quad \mathrm{I}_{-\frac{1}{2}}\left(\sqrt{\mathrm{Z}_{h_1}^{'}\lambda}\right)d\mathrm{Z}_{h_1}^{'}.\end{aligned}$$

Let $\sqrt{\lambda\mathrm{Z}_{h_1}^{'}}=x\Rightarrow\frac{\sqrt{\lambda}}{2\sqrt{\mathrm{Z}^{'}{}_{h_1}}}d\mathrm{Z}_{h_1}^{'}=dx$ then $\frac{\lambda}{2x}d\mathrm{Z}_{h_0}^{'}=dx\Rightarrow d\mathrm{Z}_{h_1}^{'}=\frac{2x}{\lambda}dx$. Rewriting the integrand

$$P_D = \frac{2}{\lambda}\int_{Z_{Th}}^{\infty}\exp\left(\frac{-\left(x^2+\lambda^2\right)}{2\lambda}\right)\sqrt{x\lambda}I_{-\frac{1}{2}}\left(x\right)dx.$$

Since $I_{-\frac{1}{2}}\left(x\right)=\sqrt{\frac{2}{\pi}}\frac{\cosh(x)}{\sqrt{x}}$, we have

$$= \frac{\sqrt{\lambda}}{\lambda}\sqrt{\frac{2}{\pi}}\int_{Z_{Th}}^{\infty}\exp\left(\frac{-\left(x^2+\lambda^2\right)}{2\lambda}\right)\sqrt{x}\frac{\cosh\left(x\right)}{\sqrt{x}}dx.$$

Since $\cosh\left(x\right)=\frac{\exp(x)+\exp(-x)}{2}$ we have

$$= \frac{\sqrt{\lambda}}{2\lambda}\sqrt{\frac{2}{\pi}}\left\{\int_{Z_{Th}}^{\infty}\exp\left(\frac{-\left(x-\lambda\right)^2}{2\lambda}\right)dx+\int_{Z_{Th}}^{\infty}\exp\left(\frac{-\left(x+\lambda\right)^2}{2\lambda}\right)dx\right\}.$$

Since $\frac{d\mathrm{erf}(y)}{dx}=2\frac{\exp\left(-y^2\right)}{\sqrt{\pi}}$ it can be shown that $\int_{Z_{Th}}^{\infty}\exp\left(-\frac{y^2}{n}\right)dy=\frac{\sqrt{\pi}}{2}\sqrt{n}\mathrm{erf}\left(\frac{x}{\sqrt{n}}\right)$. So for the first integral we have $y=\lambda-x\Rightarrow dx=-dy$, as a result the first integral can be evaluated as

$$\begin{aligned}-\int_{Z_{Th}}^{\infty}\exp\left(\frac{y^2}{2\lambda}\right)dy &= -\frac{\sqrt{\pi}}{2}\sqrt{2\lambda}\mathrm{erf}\left(\frac{\mathrm{y}}{\sqrt{2\lambda}}\right)\\ &= -\sqrt{\frac{\pi}{2}}\sqrt{\lambda}\mathrm{erf}\left(\frac{\lambda-x}{\sqrt{2\lambda}}\right).\end{aligned}$$

The second integral can be similarly evaluated as $\sqrt{\frac{\pi}{2}}\sqrt{\lambda}\mathrm{erf}\left(\frac{\lambda+x}{\sqrt{2\lambda}}\right)$ by choosing $y = \lambda + x$. Therefore we have

$$\begin{aligned} P_{_D} &= \frac{\sqrt{\lambda}}{2\lambda}\sqrt{\frac{2}{\pi}}\sqrt{\frac{\pi}{2}}\sqrt{\lambda}\left(\mathrm{erf}\left(\frac{\lambda+x}{\sqrt{2\lambda}}\right)-\mathrm{erf}\left(\frac{\lambda-x}{\sqrt{2\lambda}}\right)\right) \\ &= 1-\frac{\mathrm{erf}\left(\sqrt{\frac{Z_{Th}}{2}}-\sqrt{\frac{\lambda}{2}}\right)+\mathrm{erf}\left(\sqrt{\frac{Z_{Th}}{2}}+\sqrt{\frac{\lambda}{2}}\right)}{2}. \end{aligned}$$

C. Derivation of mean and variance of Z_{h_0} and Z_{h_1} for scenario B (one pilot bit)

$$\begin{aligned} \mathrm{E}\left[\mathrm{Z}_{h_0}\right] &= \mathrm{E}\left[\mathrm{A}\right]\mathrm{E}\left[\sum_{i=1}^{L}\left(x_{i-\tau}x_{i-j}\right)\right]+ \\ &\quad \mathrm{E}\left[\sum_{i=1}^{L}\left(n_i x_{i-j}\right)\right]=0 \end{aligned}$$

$$\begin{aligned} \mathrm{Var}\left[\mathrm{Z}_{h_0}\right] &= \mathrm{Var}\left[\mathrm{X}_{h_0}\right]+\mathrm{Var}\left[\mathrm{N}\right] \\ &= 0+\frac{L}{4}\frac{b^2\pi}{2}+\frac{L}{4}\frac{b^2\left(4-\pi\right)}{2}+L\sigma_n^2 \\ &= \frac{L}{2}\left(b^2+\sigma_n^2\right) \end{aligned}$$

$$\begin{aligned} \mathrm{E}\left[\mathrm{Z}_{h_1}\right] &= \mathrm{E}\left[\mathrm{A}\right]\mathrm{E}\left[\sum_{i=1}^{L}\left(x_{i-j}x_{i-j}\right)\right]+\mathrm{E}\left[\mathrm{N}\right] \\ &= \mathrm{E}\left[\mathrm{A}\right]\mathrm{E}\left[\mathrm{X}_{h_1}\right]+\mathrm{E}\left[\mathrm{N}\right]=\frac{Lb}{2}\sqrt{\frac{\pi}{2}}. \end{aligned}$$

$$\begin{aligned} \mathrm{Var}\left[\mathrm{Z}_{h_1}\right] &= \mathrm{Var}\left[\mathrm{X}_{h_1}\right]+\mathrm{Var}\left[\mathrm{N}\right] \\ &= \frac{L^2b^2}{8}\left(4-\pi\right)+\frac{L}{2}\sigma_n^2. \end{aligned}$$

D. Derivation of mean and variance of Z_{h_0} and Z_{h_1} for scenario C

$$\begin{aligned} \mathrm{E}\left[\mathrm{Z}_{h_0}\right] &= \mathrm{E}\left[\sum_{i=1}^{L}\left(a_i x_{i-\tau}x_{i-j}\right)\right]+\mathrm{E}\left[\sum_{i=1}^{L}\left(n_i x_{i-j}\right)\right] \\ &= =0 \end{aligned}$$

$$\begin{aligned} \mathrm{Var}\left[\mathrm{Z}_{h_0}\right] &= \mathrm{Var}\left[\sum_{i=1}^{L}\left(a_i x_{i-\tau}x_{i-j}\right)\right]+ \\ &\quad \mathrm{Var}\left[\sum_{i=1}^{L}\left(n_i x_{i-j}\right)\right] \\ &= \frac{Lb^2}{2}+\frac{L\sigma_n^2}{2}. \end{aligned}$$

$$\begin{aligned} \mathrm{E}\left[\mathrm{Z}_{h_1}\right] &= \mathrm{E}\left[\sum_{i=1}^{L}a_i\left(x_{i-\tau}^2\right)\right]+\mathrm{E}\left[\sum_{i=1}^{L}\left(n_i x_{i-j}\right)\right] \\ &= \frac{Lb}{2}\sqrt{\frac{\pi}{2}}. \end{aligned}$$

$$\begin{aligned} \mathrm{Var}\left[\mathrm{Z}_{h_1}\right] &= \mathrm{Var}\left[\sum_{i=1}^{L}\left(x_{i-j}x_{i-j}\right)\right]+ \\ &\quad \mathrm{Var}\left[\sum_{i=1}^{L}\left(n_i x_{i-j}\right)\right] \\ &= L\left\{\frac{b^2\left(6-\pi\right)+4\sigma_n^2}{8}\right\}. \end{aligned}$$

ACKNOWLEDGMENT

The authors would like to thank Prof. Giulio Colavolpe, the editor for IEEE Transactions on Wireless Communications, and the anonymous reviewers for their constructive comments regarding the manuscript.

REFERENCES

[1] U. Parlitz, L. Chua, K. Halle, L. Kocarev, and A. Shang, "Transmission of digital signals by chaotic synchronization," *International J. Bifurcation Chaos Appl. Sci. Eng.*, vol. 2, no. 4, pp. 973–977, 1992.

[2] G. Kolumban, M. P. Kennedy, and L. O. Chua, "The role of synchronization in digital communications using chaos—I: fundamentals of digital communications," *IEEE Trans. Circuits Syst. I*, vol. 44, no. 10, pp. 927–936, Oct. 1997.

[3] T. Kohda, Y. Matsumura, and Y. Jitsumatsu, "Bit error rate in an asynchronous DS/CDMA system using Markovian SS codes," vol. 2, 2002, pp. 571–575.

[4] G. Mazzini, R. Rovatti, and G. Setti, "Chaos-based asynchronous DS-CDMA systems and enhanced Rake receivers: measuring the improvements," *IEEE Trans. Circuits Syst. I*, vol. 48, no. 12, pp. 1445–1453, Dec. 2001.

[5] H. Dedieu, M. Kennedy, and M. Hasler, "Chaos shift keying: modulation and demodulation of a chaotic carrier using self-synchronizing Chua's circuits," *IEEE Trans. Circuits Syst. I Analog Digital Signal Process.*, vol. 40, no. 10, pp. 634–642, Oct. 1993.

[6] L. Kocarev, K. S. Halle, K. Echert, L. Chua, and U. Parlitz, "Experimental demonstration of secure communicaions via chaotic synchronization," *International J. Bifurcation Chaos Appl. Sci. Eng.*, vol. 2, no. 3, pp. 709–713, 1992.

[7] R. Vali, S. Berber, and S. Nguang, "Effect of Rayleigh fading on non-coherent sequence synchronization for multi-user chaos based DS-CDMA," *Signal Process.*, vol. 90, no. 6, pp. 1924–1939, 2010.

[8] R. Vali, S. Berber, and S. K. Nguang, "Analysis of a chaos-based non-coherent delay lock tracking loop," in *Proc. IEEE International Conf. Commun.*, pp. 1–6.

[9] ——, *Planning and Optimisation of 3G and 4G Wireless Networks*. River Publishers, 2009, ch. Synchronization, pp. 445–479.

[10] W. M. Tam, F. C. M. Lau, and C. K. Tse, "A multiple access scheme for chaos-based digital communication systems utilizing transmitted reference," *IEEE Trans. Circuits Syst. I*, vol. 51, no. 9, pp. 1868–1878, Sep. 2004.

[11] W. Tam, F. Lau, C. Tse, and A. Lawrance, "Exact analytical bit error rates for multiple access chaos-based communication systems," *IEEE Trans. Circuits Syst. II*, vol. 51, no. 9, pp. 473–481, Sep. 2004.

[12] A. Kurian, S. Puthusserypady, and S. M. Htut, "Performance enhancement of DS/CDMA system using chaotic complex spreading sequence," *IEEE Trans. Wireless Commun.*, vol. 4, no. 3, pp. 984–989, May 2005.

[13] J. Yao and A. Lawrance, "Performance analysis and optimization of multi-user differential chaos-shift keying communication systems," *IEEE Trans. Circuits Syst. I*, vol. 53, no. 9, pp. 2075–2091, Sep. 2006.

[14] G. Kolumban, M. P. Kennedy, and L. O. Chua, "The role of synchronization in digital communications using chaos—II: chaotic modulation and chaotic synchronization," *IEEE Trans. Circuits Syst. I*, vol. 45, no. 11, pp. 1129–1140, Nov. 1998.

[15] G. Mazzini, G. Setti, and R. Rovatti, "Chaotic complex spreading sequences for asynchronous DS-CDMA—I: system modeling and results," *IEEE Trans. Circuits Syst. I*, vol. 44, no. 10, pp. 937–947, Oct. 1997.

[16] R. Rovatti, G. Setti, and G. Mazzini, "Chaotic complex spreading sequences for asynchronous DS-CDMA—part II: some theoretical performance bounds," *IEEE Trans. Circuits Syst. I*, vol. 45, no. 4, pp. 496–506, Apr. 1998.

[17] F. Lau and C. Tse, *Chaos-Based Digital Communicaion Systems*. Springer, 2004.

[18] G. Heidari-Bateni and C. D. McGillem, "A chaotic direct-sequence spread-spectrum communication system," *IEEE Trans. Commun.*, vol. 42, no. 234, pp. 1524–1527, Feb. 1994.
[19] R. Rovatti, G. Setti, and G. Mazzini, "Chaos-based spreading compared to M-sequences and Gold spreading in asynchronous CDMA communication systems," in *Proc. 1997 European Conf. Circuit Theory Design*.
[20] G. Setti, R. Rovatti, and G. Mazzini, "Performance of chaos-based asynchronous DS-CDMA with different pulse shapes," *IEEE Commun. Lett.*, vol. 8, no. 7, pp. 416–418, July 2004.
[21] M. Hasler and T. Schimming, "Optimal and suboptimal chaos receivers," *Proc. IEEE*, vol. 90, no. 5, pp. 733–746, May 2002.
[22] T. Schimming and M. Hasler, "Optimal detection of differential chaos shift keying," *Circuits Syst. I: Fundamental Theory Appl., IEEE Trans.*, vol. 47, no. 12, pp. 1712–1719, Dec. 2000.
[23] G. Kolumban, M. P. Kennedy, and L. O. Chua, "The role of synchronization in digital communications using chaos—III: performance bounds for correlation receivers," *IEEE Trans. Circuits Syst. I*, vol. 47, no. 12, pp. 1673–1683, Nov. 2000.
[24] M. P. Kennedy, R. Rovatti, and G. Setti, *Chaotic Electronics in Telecommunications*. CRC Press, 2000.
[25] U. Parlitz and S. Ergezinger, "Robust communication based on chaotic spreading sequences," *Physics Lett. A*, vol. 188, no. 2, pp. 146–150, 1994.
[26] A. Polydoros, "On synchronization aspects of direct-sequence spread spectrum systems," Ph.D. dissertation, University of Southern California, Los Angeles, 1982.
[27] Y. K. T. Eshima and N. Jitsumatsu, "Markovian SS codes imply inversion-free code acquisition in asynchronous DS/CDMA systems," vol. 4, pp. IV-617–IV-620, May 2004.
[28] N. Eshima and T. Kohda, "Statistical approach to the code acquisition problem in direct-sequence spread-spectrum communication systems," *IMA J. Math. Control Inf.*, vol. 23, no. 2, pp. 149–163, 2006.
[29] Y. Jitsumatsu, N. Eshima, and T. Kohda, "Code acquisition of Markovian SS codes in a chip-synchronous DS-CDMA system," 29 June-4 July 2003, p. 447.
[30] T. A. Khan, N. Eshima, Y. Jitsurnatsu, and T. Kohda, "Multiuser code acquisition in DS/CDMA systems," in *Proc. 2003 IEEE Topical Conf. Wireless Commun. Technol.*, pp. 121–122.
[31] T. Kohda, Y. Jitsumatsu, and T. Khan, "Spread-spectrum Markovian-code acquisition in asynchronous DS/CDMA systems," in *Proc. 2003 International Symposium on Circuits and Systems*, vol. 3, pp. 750–753.
[32] B. Jovic, C. Unsworth, G. Sandhu, and S. Berber, "A robust sequence synchronization unit for multi-user DS-CDMA chaos-based communication systems," *Signal Process.*, vol. 87, no. 7, pp. 1692–1708, 2007.
[33] B. Jovic, "Synchronisation techniques for single and multiple-access chaotic communication systems," Ph.D. dissertation, Faculty of Engineering, The University of Auckland, 2007.
[34] B. Jovic and C. Unsworth, "Fast synchronisation of chaotic maps for secure chaotic communications," *Electron. Lett.*, vol. 46, no. 1, pp. 49–50, 2010.
[35] G. Kaddoum, D. Roviras, P. Charge, and D. Fournier-Prunaret, "Robust synchronization for asynchronous multi-user chaos-based DS-CDMA," *Signal Process.*, vol. 89, no. 5, pp. 807–818, 2009.
[36] G. Setti, R. Rovatti, and G. Mazzini, "Synchronization mechanism and optimization of spreading sequences in chaos-based DS-CDMA systems," *IEICE Trans. Fundamentals Electron., Commun. Comput. Sci.*, vol. E82-A, no. 9, pp. 1737–1746, Sep. 1999.
[37] G. Mazzini, R. Rovatti, and G. Setti, "Sequence synchronization in chaos-based DS-CDMA systems," in *Proc. 1998 IEEE International Symp. Circuits Syst.*, vol. 4, pp. 485–488.
[38] G. Setti, G. Mazzini, and R. Rovatti, "Gaussian characterization of self-interference during synchronization of chaos based DS-CDMA systems," in *Proc. 1998 IEEE International Conf. Electron., Circuits Syst.*, vol. 1, pp. 231–234.
[39] S. Berber and B. Jovic, "Sequence synchronization in a wideband CDMA system," in *Proc. 2006 International Conf. Wireless Broadband Ultra Wideband Commun.*, pp. 1–6.
[40] M. C. Jeruchim, P. Balaban, and K. S. Shanmugan, *Simulation of Communication Systems: Modeling, Methodology and Techniques*, M. C. Jeruchim, P. Balaban, and K. S. Shanmugan, editors. Kluwer Academic Publishers, 2000.
[41] T. Geisel and V. Fairen, "Statistical properties of chaos in Chebyshev maps," *Physics Lett.*, vol. 105A, pp. 263–266, 1984.
[42] G. Kaddoum, P. Chargé, D. Roviras, and D. Fournier-Prunaret, "A methodology for bit error rate prediction in chaos-based communication systems," *Circuits, Systems, and Signal Processing*. Available: http://dx.doi.org/10.1007/s00034-009-9124-5
[43] R. L. Peterson, R. E. Zeimer, and D. E. Borth, *Introduction to Spread Spectrum Communicaion*. Prentice Hall, 1995.
[44] E. Biglieri, G. Caire, and G. Taricco, "Coding for the fading channel: a survey," *Signal Process.*, vol. 80, no. 7, pp. 1135–1148, 2000.
[45] M. K. Simon, *Probability Distributions Involving Gaussian Random Variables*. Springer, 2002.
[46] N. Johnson and H. Tetley, *Statistics: An Intermediate Textbook, Vol. 1*. Cambridge University Press, 1949.
[47] E. Biglieri, J. Proakis, and S. Shamai, "Fading channels: information-theoretic and communications aspects," *IEEE Trans. Inf. Theory*, vol. 44, no. 6, pp. 2619–2692, Oct. 1998.

Ramin Vali received the BE degree (honours) from the Department of Electrical and Computer Engineering, The University of Auckland, New Zealand in 2007. Currently, he is with the same department as a PhD candidate. He has published a number of peer reviewed conference and journal papers in the field of chaos-based spread spectrum communication systems. He has also been a reviewer for the IEEE TRANSACTIONS ON WIRELESS COMMUNICATIONS. His research interests include: spread spectrum security, chaos-based communication systems and their synchronisation, chaos-based CDMA, LTE and OFDM communication systems.

Stevan Mirko Berber was born in Stanisic, Serbia, former Yugoslavia. He completed his undergraduate studies in electrical engineering in Zagreb, master studies in Belgrade, and PhD studies in Auckland, New Zealand. Currently Stevan is with the Department of Electrical and Computer Engineering at Auckland University, New Zealand. He was appointed Visiting Professor at the University of Novi Sad in 2004 and Visiting Scholar at the University of Sydney in 2008. His teaching interests are in communication systems, information and coding theory, discrete stochastic signal processing and wireless sensor and computer networks. His research interests are in the fields of digital communication systems and signal processing with the emphasis on applications in CDMA systems and wireless computer, communication and sensor networks. He is the author of more than 80 refereed journal and conference papers, 8 books and three book chapters. Dr Berber is a referee for papers in leading journals and conferences in his research area. He has been leading or working on a large number of research and industry projects. Dr. Berber is a senior member of IEEE, a member of New Zealand Scientists, and an accredited NAATI translator for English language.

Sing Kiong Nguang received the B.E. (with first class honours) and the Ph.D. degree from the Department of Electrical and Computer Engineering of the University of Newcastle, Australia, in 1992 and 1995, respectively. Currently, he is with the Department of Electrical and Computer Engineering, University of Auckland, Auckland, New Zealand. He has published over 200 refereed journal and conference papers on nonlinear control design, nonlinear control systems, nonlinear time-delay systems, nonlinear sampled-data systems, biomedical systems modelling, fuzzy modelling and control, biological systems modelling and control, and food and bioproduct processing. He has/had served on the editorial board of a number of international journals. He is the Chief-Editor of the *International Journal of Sensors, Wireless Communications and Control*.